

## Relating Seasonal Patterns of the AVHRR Vegetation Index to Simulated Photosynthesis and Transpiration of Forests in Different Climates

STEVEN W. RUNNING AND RAMAKRISHNA R. NEMANI

*School of Forestry, University of Montana, Missoula, Montana 59812*

Recent research has suggested that the Normalized Difference Vegetation Index (NDVI) calculated from the AVHRR sensor is directly related to photosynthesis (PSN), transpiration (TRAN), and aboveground net primary production (ANPP) of terrestrial vegetation. Weekly NDVI data for 1983-1984 were retrieved for seven sites of diverse climate in North America. The sites were Fairbanks, AK, Seattle, WA, Missoula, MT, Madison, WI, Knoxville, TN, Jacksonville, FL, and Tucson, AZ. Meteorological data from ground stations were retrieved to drive an ecosystem simulation model (FOREST-BGC) calculating daily canopy PSN and TRAN and annual ANPP of a hypothetical forest stand for the corresponding period at each site. Correlations of annual integrated NDVI across all sites for both years were: annual PSN,  $R^2 = 0.87$ ; annual TRAN,  $R^2 = 0.77$ ; annual ANPP,  $R^2 = 0.72$ . Correlation between weekly NDVI and PSN was variable: with high latitude wet sites,  $R^2 = 0.77-0.84$ . On sites with less seasonal amplitude of NDVI and PSN, or on sites with substantial seasonal water stress correlations ranged from  $R^2 = 0.08$  to 0.64. Correlations of weekly NDVI with TRAN followed the same pattern as PSN, but were slightly lower. The tendency of raw NDVI data to overpredict PSN and TRAN on water limited sites was partially corrected using an "aridity index" of annual radiation/annual precipitation that could be computed from general climatological data for improving large scale NDVI maps of PSN and TRAN. The spatial subsampling done for the global vegetation index (GVI) precludes following specific study sites through the growing season. We conclude that estimates of vegetation productivity using the GVI should only be done as annual integrations until unsampled local area coverage (LAC) NDVI data can be tested against forest PSN, TRAN, and ANPP, measured at shorter time intervals.

### Introduction

The photosynthetic fixation of  $\text{CO}_2$  by terrestrial vegetation is a major variable in the global carbon budget (Emmanuel et al., 1984). Major questions in global ecology require understanding of how carbon and water exchange rates of terrestrial vegetation may react to changing global climate, regional air pollution, periodic drought, and other perturbations (Dahlman, 1985). Estimates of terrestrial primary productivity could provide a regular bioassay of global habitability if means of routine estimation of photosynthetic rates and respiration were possible (Wittwer, 1983).

Regular satellite coverage of global vegetation provides the only practical means of making these estimations over global scales. The AVHRR (Advanced Very High Resolution Radiometer) sensor flown on the NOAA meteorological satellites has been used increasingly in recent years to analyze regional and global vegetation by calculating the normalized difference vegetation index (NDVI), generated by  $(\text{NIR}-\text{R})/(\text{NIR}+\text{R})$  ratioing of Channels 1 ( $\text{R} = 0.58-0.68 \mu\text{m}$ ) and 2 ( $\text{NIR} = 0.73-1.1 \mu\text{m}$ ). Initial applications of the NDVI were to map regional and then global land cover, and follow seasonal changes in greenness (Tucker et al., 1985; Justice et al., 1985). A theoretical

comparison of the NDVI with photosynthesis and transpiration models suggested that for vegetation experiencing optimal temperature and water availability the NDVI may be directly related to canopy  $\text{CO}_2$  and  $\text{H}_2\text{O}$  exchange activity and canopy conductance (Sellers, 1985; 1987).

Current research continues to explore the ability of the NDVI to go beyond vegetation cover mapping to actually estimating functional attributes of vegetation such as photosynthetic rates, evapotranspiration, and net primary productivity. Goward et al. (1985) and Goward and Dye (1987) used the seasonal integration of NDVI as an estimate of annual NPP in natural vegetation. Tucker et al. (1986) and Fung et al. (1987) have related the seasonal trend of NDVI to the annual oscillation of global atmospheric  $\text{CO}_2$  concentration, implying a link between the NDVI and photosynthetic, respiration, and decomposition activity.

The objective of this paper is to test the hypothesis that seasonal trends of NDVI can represent seasonal rates of photosynthesis and transpiration of natural forest cover in widely contrasting environments. Further, does the annual integration of NDVI correlate well with annual NPP as suggested by Goward et al. (1985) and Goward and Dye (1987)? How far can the prediction of Sellers (1985; 1987) that NDVI is directly related to PSN and TRAN be extrapolated, especially as environmental conditions diverge from optimality? Because direct measurement of forest photosynthesis of land areas of the aggregated NDVI pixel size ( $15 \times 15$  km) is impossible, we will compare the NDVI against simulation results from a process level ecosystem model of canopy  $\text{CO}_2$  and  $\text{H}_2\text{O}$  exchange,

FOREST-BGC, that has been developed from recent ecosystem analysis modeling research (Running and Coughlan, 1987; Running, 1984).

This study was executed for seven sites in North America representing a wide range of annual climates: Jacksonville, FL, representing a hot, wet climate; Knoxville, TN, warm, wet; Seattle, WA, cool, wet; Madison, WI, cool, wet; Missoula, MT, cool, dry; Fairbanks, AK, cold, dry; and Tucson, AZ, hot, dry. At each site NDVI data was extracted for 1983 and 1984, and meteorological records were gathered to run the FOREST-BGC model for the same period simulating photosynthesis and transpiration of a forest in that environment.

## Methods

### NDVI data

The NOAA Satellite Data Services Division produces a global vegetation index (GVI) each week. Briefly, the GVI spatial subsampling first averages four out of five LAC (Local Area Coverage) 1.1 km pixels in one out of every three data lines to produce a  $4 \times 4$  km GAC (Global Area Coverage) average. After the NDVI channel ratio of  $(\text{Ch}2 - \text{Ch}1)/(\text{Ch}2 + \text{Ch}1)$  is calculated for each GAC pixel, the results are mapped onto a polar stereographic grid. The GVI algorithm then subsamples (randomly for these data) only one  $4 \times 4$  GAC pixel out of every  $15 \times 15$  km (at equator) on the grid, representing a final subsampling that is less than 1% of the real ground area at midlatitudes. Temporally, the highest NDVI value of each 7 day period is retained as the weekly NDVI value for that GVI cell, a compositing that reduces data variability caused by water vapor, haze, aerosols,

TABLE 1 Location of the GVI Cells and Forest Type for the Seven Study Sites

SITE	LATITUDE (°N)	LONGITUDE (°W)	FOREST TYPE
Fairbanks, AK	64.45	148.15	spruce-hardwood
Seattle, WA	46.00	122.00	Douglas-fir
Missoula, MT	47.00	113.33	ponderosa pine
Madison, WI	43.40	89.45	oak-hickory
Knoxville, TN	36.27	84.00	oak-pine
Jacksonville, FL	30.00	82.00	longleaf-slash pine
Tucson, AZ	32.00	110.00	P. pine-chaparral

sun angle, and sensor look angle. Details of these rather complicated sampling methods can be found in Tarpley et al. (1984), Kidwell (1984), Malingreau (1986), and Holben (1986).

We obtained weekly GVI data for weeks 10–52 of 1983 and all of 1984. At each of the seven study areas we extracted the GVI cell with the highest NDVI to avoid unvegetated areas and be reasonably confident of imaging forested land, which would have the highest LAI. However, we cannot be sure that some component of grassland or agricultural crops with high NDVI value may be part of these cells. The exact location of each sample GVI cell and general forest type is given in Table 1. An important consequence, for this study, of the rather complicated spatial and temporal subsampling is that one cannot locate a specific forest stand for purposes of defining site and stand attributes such as leaf area index or soil depth for modeling or validation purposes.

#### FOREST-BGC model

FOREST-BGC (*BioGeochemical Cycles*) is a process level ecosystem simulation model that calculates the cycling of carbon, water, and nitrogen through forest ecosystems. A flowchart of the model, illustrating carbon, water and nitrogen state variables is shown in Fig. 1. The

model requires daily input data of standard meteorological conditions, maximum–minimum air temperature, dew point, incident shortwave radiation and precipitation, and definition of key site and vegetation variables (see Tables 2 and 3.) The model calculates key processes of canopy interception and evaporation, transpiration, soil outflow of water; photosynthesis, growth and maintenance respiration, allocation, litterfall and decomposition of carbon; and deposition, uptake, litterfall, and mineralization of nitrogen. The model has a mixed time resolution, with hydrologic, photosynthetic, and maintenance respiration processes computed daily, and the other carbon and all nitrogen processes computed yearly.

For this study the important parts of the model are the hydrologic balance, evapotranspiration and canopy water stress, and photosynthesis. Briefly, daily precipitation is routed to snowpack or soil dependent on air temperature, a canopy interception fraction based on LAI is subtracted and evaporated, and remaining water goes to a soil compartment where it is available for transpiration. Transpiration is calculated with a Penman–Monteith equation incorporating both radiation and vapor pressure deficit drivers for the process. The canopy conductance term is a complex function of air temperature, vapor pressure deficit,

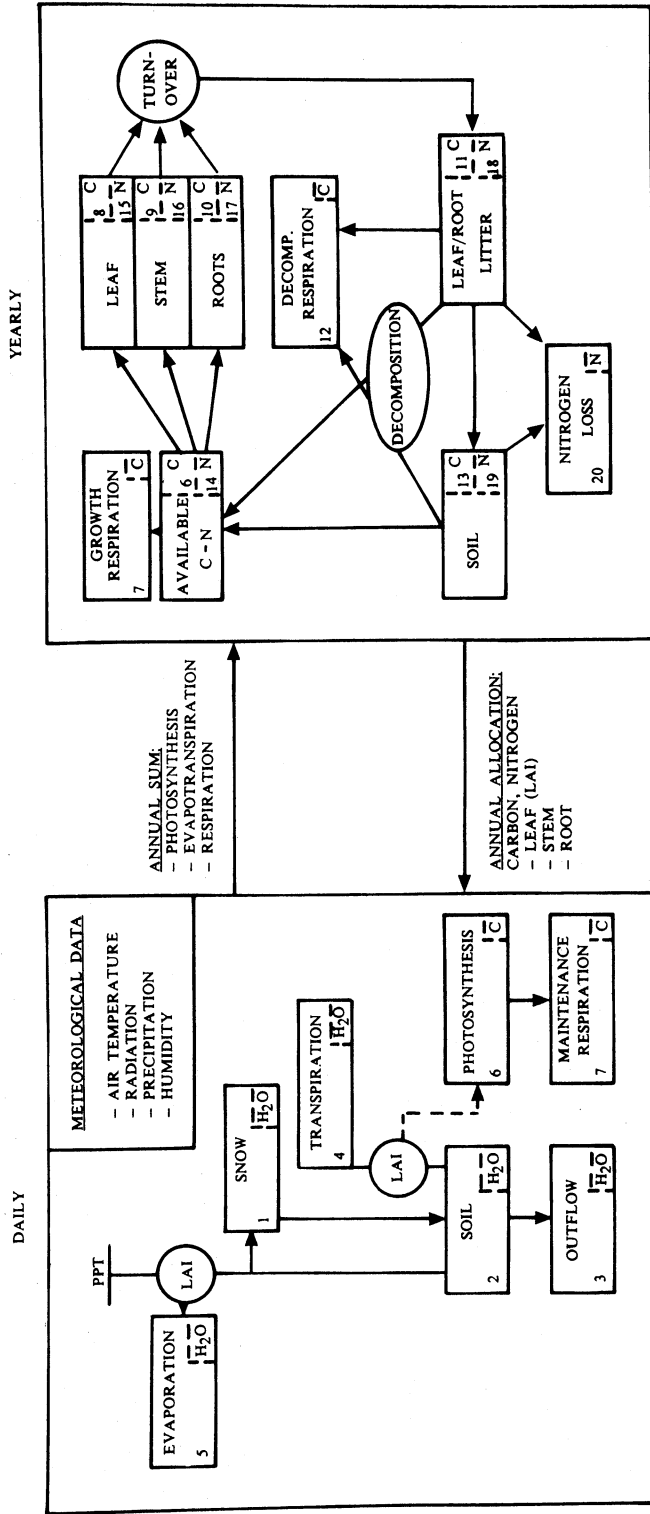


FIGURE 1. A compartment flow diagram of the ecosystem simulation model FOREST-BCC. This model calculates cycling of carbon, water, and nitrogen through forest ecosystems and is designed for compatibility with remote sensing data sources.

**TABLE 2A** Driving and Derived Environmental Variables for FOREST-BGC

Z	DESCRIPTION
1	year
2	yearday
3	precipitation (mm)
4	maximum air temperature (°C)
5	minimum air temperature (°C)
6	relative humidity (%)
7	soil temperature, av. 24 h temp (°C)
8	shortwave radiation (kJ/m <sup>2</sup> /day)
10	leaf area index (m <sup>2</sup> /m <sup>2</sup> )
14	daylight average air temperature (°C)
15	average night minimum temperature (°C)
16	vapor pressure deficit (mb)
17	absolute humidity deficit (μg/m <sup>3</sup> )
18	daylength (s)
19	canopy daily av. radiation (kJ/m <sup>2</sup> /day)
21	leaf nitrogen concentration (%)

**TABLE 2B** Intermediate Variables Calculated in FOREST-BGC

G	DESCRIPTION
1	rain—canopy interception (m/day)
2	snow (m/day)
3	snowmelt (m/day)
4	potential evaporation of precipitation (m/day)
5	potential evaporation radiation limits (m/day)
6	potential PPT, evap.—energy limited potential evap. (m/day)
10	soil—predawn leaf water potential ( - MPa)
11	canopy H <sub>2</sub> O conductance, soil water control (m/s)
12	canopy H <sub>2</sub> O conductance night minimum temp. reduction (m/s)
13	canopy H <sub>2</sub> O conductance humidity deficit reduction (m/s)
14	canopy H <sub>2</sub> O conductance radiation reduction (m/s)
15	final canopy H <sub>2</sub> O conductance (m/s)
16	Penman-Monteith transpiration (m H <sub>2</sub> O/LAI/s)
17	canopy transpiration (m H <sub>2</sub> O/day)
18	ground water outflow (m H <sub>2</sub> O/day)
19	canopy % nitrogen control on CO <sub>2</sub> conductance (multiplier)
20	light effect on CO <sub>2</sub> conductance (multiplier)
21	temp. effect on CO <sub>2</sub> conductance (multiplier)
22	final mesophyll CO <sub>2</sub> conductance (m/s)
23	gross photosynthesis (kg/LAI)
24	daily gross photosynthesis (kg/day)
25	night canopy respiration (kg/day)
26	24 h net carbon fixation (kg/day)
30	stem maintenance respiration (kg/day)
31	root maintenance respiration (kg/day)
50	carbon allocation to canopy (%)
51	carbon allocation to stem (%)
52	carbon allocation to roots (%)
54	canopy growth respiration (kg/year)
55	stem growth respiration (kg/year)
56	root growth respiration (kg/year)
57	canopy growth (kg/year)
58	stem growth (kg/year)
59	root growth (kg/year)
60	canopy litterfall (kg/year)
61	stem litterfall (kg/year)
62	root litterfall (kg/year)

TABLE 3 Initial Conditions and Parameter Values for Simulations, Using the Missoula, MT Site as an Example<sup>a</sup>

VALUE	VARIABLE	DESCRIPTION	UNITS
<u>Initial Conditions</u>			
534.0	X(1)	snowpack	(m <sup>3</sup> )
452.0	X(2)	soil water content	(m <sup>3</sup> )
0.0	X(3)	water outflow	(m <sup>3</sup> )
0.0	X(4)	transpiration	(m <sup>3</sup> )
0.0	X(5)	evaporation	(m <sup>3</sup> )
0.0	X(6)	PSN	(kg)
0.0	X(7)	respiration autotrophic	(kg)
2.40E+3	X(8)	leaf carbon	(kg)
50.0E+3	X(9)	stem carbon	(kg)
25.0E+3	X(10)	root carbon	(kg)
<u>Input Parameters</u>			
25.0	B(1)	specific leaf area	(m <sup>2</sup> /kg °C)
0.5	B(2)	canopy light extinction coefficient	(dim)
2350.0	B(3)	soil water capacity	(m <sup>3</sup> )
0.0005	B(4)	interception coefficient	(m/LAI/day)
1.0E+4	B(5)	ground surface area	(m <sup>2</sup> /ha)
0.0007	B(6)	snowmelt coefficient	(m/°C/day)
46.	B(7)	latitude	(deg)
0.80	B(8)	l-surface albedo	(dim)
0.5	B(9)	spring min. LWP	(- MPa)
3000	B(10)	radiation KL threshold	(kJ/m <sup>2</sup> /day)
0.0016	B(11)	max canopy conductance, H <sub>2</sub> O	(m/s)
1.65	B(12)	LWP at stomatal closure	(- MPa)
0.05	B(13)	slope KL humidity reduction	(m/s/μg/m <sup>3</sup> )
432	B(14)	photosynthesis light compensation	(kJ/m <sup>2</sup> /day)
9720	B(15)	0.5 photosynthesis maximum	(kJ/m <sup>2</sup> /day)
0.0008	B(16)	max mesophyll conductance, CO <sub>2</sub>	(m/s)
0	B(17)	min temperature photosynthesis	(°C)
40	B(18)	max temperature photosynthesis	(°C)
0.00015	B(19)	leaf respiration coefficient	(kg/°C/day/kg)
0.0010	B(20)	stem respiration coefficient	(kg/°C/day/kg)
0.0002	B(21)	root respiration coefficient	(kg/°C/day/kg)
4.0	B(23)	temperature effect mesophyll conductance	(dim)
0.085	B(25)	Q <sub>10</sub> = 2.3 constant for exponential respiration	(dim)
0.015	B(26)	leaf nitrogen concentration	(fract)
0.25	B(30)	leaf carbon allocation fraction	(dim)
0.35	B(31)	stem carbon allocation fraction	(dim)
0.40	B(32)	root carbon allocation fraction	(dim)
0.33	B(40)	leaf litter C turnover	(fract/yr)
0.00	B(41)	stem litter C turnover	(fract/yr)
0.40	B(42)	root litter C turnover	(fract/yr)
0.35	B(43)	leaf growth respiration	(fract)
0.30	B(44)	stem growth respiration	(fract)
0.35	B(45)	root growth respiration	(fract)

<sup>a</sup>A ground area of 1 ha is implicit in the units.

incident radiation, and leaf water potential. Air temperature below 0°C reduces canopy conductance to cuticular values, and is an important determinant of the growing season length. Canopy conductance is linearly reduced to a default cuticular value when either average daily vapor pressure deficits exceed 16 mb or predawn leaf water potential, estimated from soil water availability, decreases below -1.65 MPa. Aerodynamic conductance is fixed at 0.2 m/s in the Penman-Monteith equation.

Canopy photosynthesis is calculated by multiplying a CO<sub>2</sub> diffusion gradient by a radiation and temperature controlled mesophyll CO<sub>2</sub> conductance and the canopy water vapor conductance:

$$\text{PSN} = \left[ \frac{(\text{CO}_2 * \text{KL} * \text{KM})}{(\text{KL} + \text{KM})} \right] * \text{LAI} * \text{DAYL}, \quad (1)$$

where

- PSN = canopy daily photosynthesis (kg CO<sub>2</sub>/ha/day),  
 CO<sub>2</sub> = CO<sub>2</sub> diffusion gradient from leaf to air (kg/m<sup>3</sup>),  
 KL = canopy water vapor conductance × 0.64 (m/s),  
 KM = canopy CO<sub>2</sub> mesophyll conductance (m/s),  
 LAI = leaf area index, projected (m<sup>2</sup>/m<sup>2</sup>),  
 DAYL = daylength (s/day).

The light response surface for mesophyll conductance is asymptotic with half maximum photosynthesis at 9720 kJ/m<sup>2</sup>/day. A light attenuation of -0.5/LAI is used for Beers law extinction of incident radiation to produce canopy average radiation. The inverse parabolic temperature re-

sponse surface has an optimum of 20°C, with high and low compensation points of 0 and 40°C, respectively. Aboveground net primary production (ANPP) is estimated by first subtracting 40% of PSN as root growth allocation, then subtracting a maintenance respiration term calculated as an exponential function of air temperature with a  $Q_{10} = 2.3$ , for all biomass, and third, subtracting 35% of remaining PSN as growth respiration. As the complete model is rather large, further documentation can be found in Running and Coughlan (1987).

Because the primary interest in this study is seasonal photosynthesis and transpiration, only the daily (24 h) half of the model was used, and the only output we will report is weekly summaries of PSN and TRAN and an estimate of annual ANPP. Companion simulations giving greater detail of model output of the other processes is reported in Running and Coughlan (1987).

Meteorological data for the seven study sites for 1983 and 1984 were retrieved from the monthly summary, National Weather Service Local Climatological Data of the United States. Daily records of maximum air temperature, minimum air temperature, dew point, and precipitation were retrieved from the compiled records. Incoming solar radiation was not available, so we derived these data from climatological principles of Bristow and Campbell (1984), and the program of Running et al. (1987). Briefly, this logic first calculates potential incoming radiation to a flat surface from geometric principles using latitude and yearday. Then an atmospheric transmission coefficient is computed based on site elevation, yearday, and a seasonally corrected cloudcover estimate based on daily maxi-

mum–minimum air temperature. Finally, the daily transmission coefficient is multiplied by the potential radiation to give actual incident radiation in  $\text{kJ}/\text{m}^2/\text{day}$ . This procedure has been used before by both Bristow and Campbell (1984) and Running et al. (1987) and tested to give acceptable estimates of daily radiation in both maritime and continental climates.

The only site parameter required is soil water holding capacity, which was set at 23.5 cm for all sites based on previous work (Running and Coughlan, 1987). Two canopy parameters are needed, leaf area index (LAI), defined at 6.0 total or 2.7 projected LAI for all sites, and leaf nitrogen concentration, defined at 1.5% of dry weight for all sites, each treated as constants for the year. Initial conditions of snowpack and soil water content on Yearday 1 were defined from Running and Coughlan (1987). Because the GVI sample plot for each site is so large, we consider these simulations to be general computations for a hypothetical forest at these locations, rather than a simulation of a specific forest. We only expected these simulations to illustrate the general seasonal photosynthetic and transpirational activity as related to climate.

For data analysis, 7-day summaries of photosynthesis and transpiration to match the weekly NDVI composite were scaled to the NDVI data and plotted together to aid in visual comparison of the seasonal trends. Annual summation of weekly values of NDVI, PSN, and TRAN was done and regressed against each other. Because the 1983 NDVI data started on Yearday 70, the first 9 weeks of 1984 data were added to the 1983 NDVI data to provide an accurate annual summary to compare with the 52 week model results. These 9 weeks are during the winter period of low

NDVI, so we feel the error involved in this procedure is minimal, especially for annual summaries. Next, to quantify the difference in correlation between NDVI and PSN and TRAN evident in the seasonal graphs for different sites, a regression of weekly composite NDVI against weekly summed PSN, and weekly TRAN was executed. Finally, an estimate of ANPP was calculated by FOREST-BGC for each site. However, the ANPP estimate is strongly influenced by above/below ground carbon partitioning ratios and the stand total biomass defined for calculating maintenance respiration losses. We used a 60/40% above/below ground carbon partitioning, and defined 50 MT C/ha of biomass for all sites except Tucson, which was 25 MT C/ha. While these parameters are reasonable for these forest types, we acknowledge possible errors resulting from not having measured data from specific stands.

## Results and Discussion

### Annual NDVI, photosynthesis, transpiration, primary production

The correlation found between the annual sums of weekly NDVI and daily PSN for both 1983 and 1984 on all sites is shown in Fig. 2, a remarkable  $R^2 = 0.87$ . For these results, NDVI was truncated to 0.0 whenever daily maximum air temperature was below  $0.0^\circ\text{C}$ , a common threshold for limiting physiological activity of plants. The correlation of annual PSN with the truncated NDVI data also had a  $R^2 = 0.87$ , but we consider the low temperature truncated NDVI data to have more biophysical significance, so will only use it for these results. The strength of this correlation was surprising because

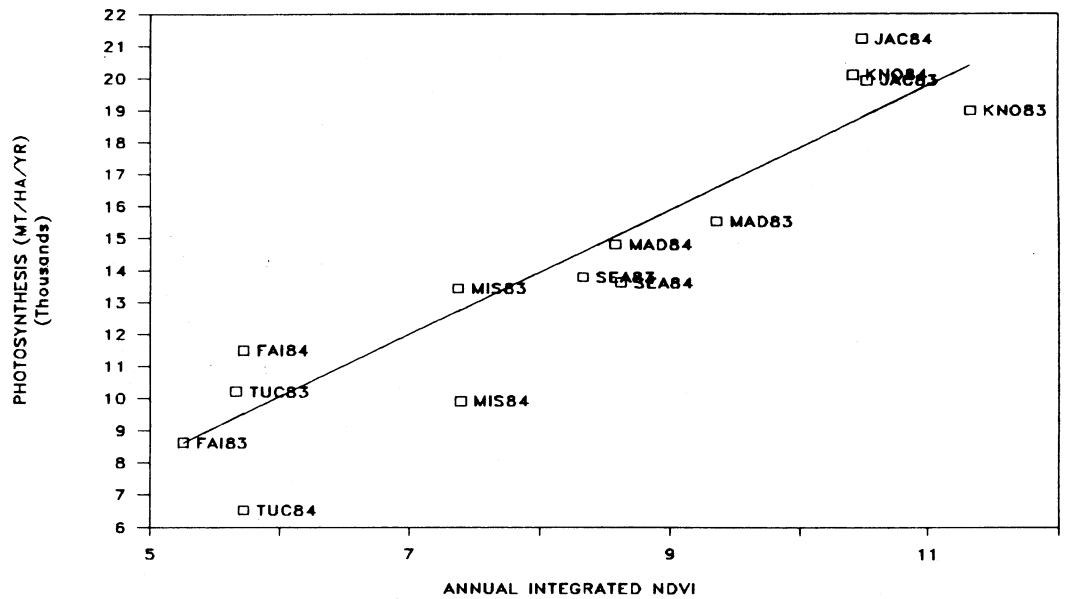


FIGURE 2. The correlation between annual integrated NDVI and annual photosynthesis (PSN) in MT carbon calculated with the FOREST-BGC model for seven sites for the years 1983 and 1984. The seven sites are Fairbanks, AK (FAI), Seattle, WA (SEA), Missoula, MT (MIS), Madison, WI (MAD), Knoxville, TN (KNO), Jacksonville, FL (JAC), and Tucson, AZ (TUC). NDVI data were weekly composite, spatially subsampled GVI data. Site climatic summaries are in Table 4. The model simulated daily photosynthesis for a hypothetical forest with projected LAI = 2.7.  $Y = 2.062X - 2.754$ .  $R^2 = 0.87$ .

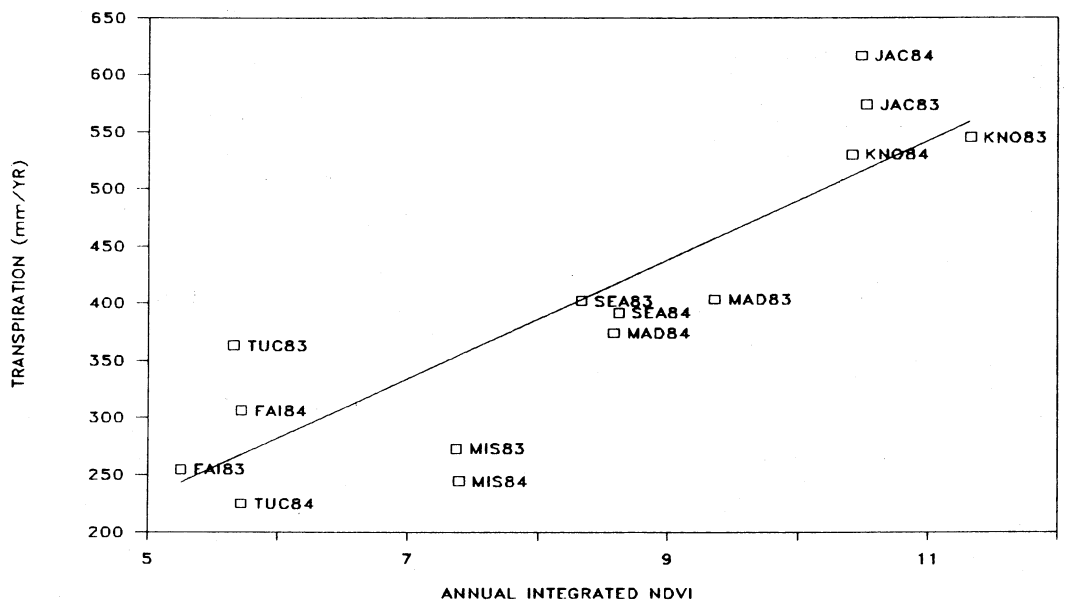


FIGURE 3. The correlation between annual integrated NDVI and annual transpiration (TRAN) in mm calculated with the FOREST-BGC model for seven sites for the years 1983 and 1984. NDVI data were weekly composite spatially subsampled GVI data. The model simulated daily transpiration for a hypothetical forest of projected LAI = 2.7.  $Y = 54.5X - 55.0$ .  $R^2 = 0.77$ .

TABLE 4 Annual Climatic Summaries for the Seven Study Sites

SITE		AIR TEMPERATURES (°C)		DEW POINT (°C)		ANNUAL RADIATION (MJ/M <sup>2</sup> /YR)	ANNUAL PRECIP (MM)
		AVERAGE JULY MAX	AVERAGE JAN MIN	AV. JULY	AV. JAN		
		Fairbanks	1983	23.1	-28.8		
	1984	21.2	-25.4	10.6	-24.5	2088	313
Seattle	1983	21.4	4.4	11.5	3.9	2460	1039
	1984	23.2	3.7	9.9	2.1	2585	939
Missoula	1983	23.7	-4.8	9.7	-6.4	4158	458
	1984	29.3	-6.9	5.8	-8.1	4232	337
Madison	1983	27.2	-13.7	15.1	-12.0	4012	843
	1984	29.9	-9.8	17.9	-8.1	3864	804
Knoxville	1983	32.1	-1.4	19.9	-0.9	4625	1078
	1984	29.0	-3.2	18.5	-3.3	4755	1231
Jacksonville	1983	33.4	2.8	22.6	4.5	4564	1579
	1984	31.3	4.5	22.1	5.5	4765	1244
Tucson	1983	38.2	4.6	10.2	-0.9	5811	555
	1984	35.9	3.8	16.0	-0.4	5909	394

the compositing used for the weekly NDVI measurement retains only the clearest day with highest radiation conditions conducive to a maximum photosynthetic potential for each week. In contrast, the FOREST-BGC model calculated PSN under the full range of daily meteorological conditions that occurred each week. An extreme scenario might be a week with heavy cloudcover for 6 days and clear the seventh. The NDVI composite would represent the clear day only, while the FOREST-BGC model would calculate radiation limited PSN rates for 6 days out of the 7. Of course, the NDVI compositing also removes daily variation in sensor view angle, a factor unrelated to surface photosynthetic potential.

The regression between integrated NDVI and annual transpiration (TRAN) is also strong, with  $R^2 = 0.77$  (Fig. 3). This result is also stronger than expected because these sites exhibit a large range in hydrologic partitioning. The transpiration/evaporation/outflow ratio ranged from 85/15/0% in Fairbanks to 43/17/40% in Seattle, across a range of annual precipitations (Table 4).

Annual net primary production (NPP) is of great interest ecologically, and has previously been related to integrated NDVI by Goward et al. (1985). The FOREST-BGC model estimated above-ground NPP (ANPP) ranging from 0 to 14.3 MT/ha/yr dry weight biomass across the seven sites (Fig. 4), very close to the ranges of <1 to 13 MT/ha/yr of NPP used by Goward et al. (1985) relating integrated NDVI to NPP across the biomes of North America. Note that FOREST-BGC calculates a range of ANPP *within* some forest biomes equal to the range *across* biomes used by Goward et al. ANPP is more closely related to climate than biome type (Webb et al., 1983). The six points of highest variability in Fig. 4 are Fairbanks, Missoula, and Tucson for 1983 and 1984. These sites had the lowest annual integrated NDVI, between 5.66 and 7.39, and large variability between 1983 and 1984 in ANPP, 35–60%, a consequence of annual variations in precipitation and temperature (Table 4). Yet there was less than 10% variability in NDVI between the two years. We feel it is not coincident-

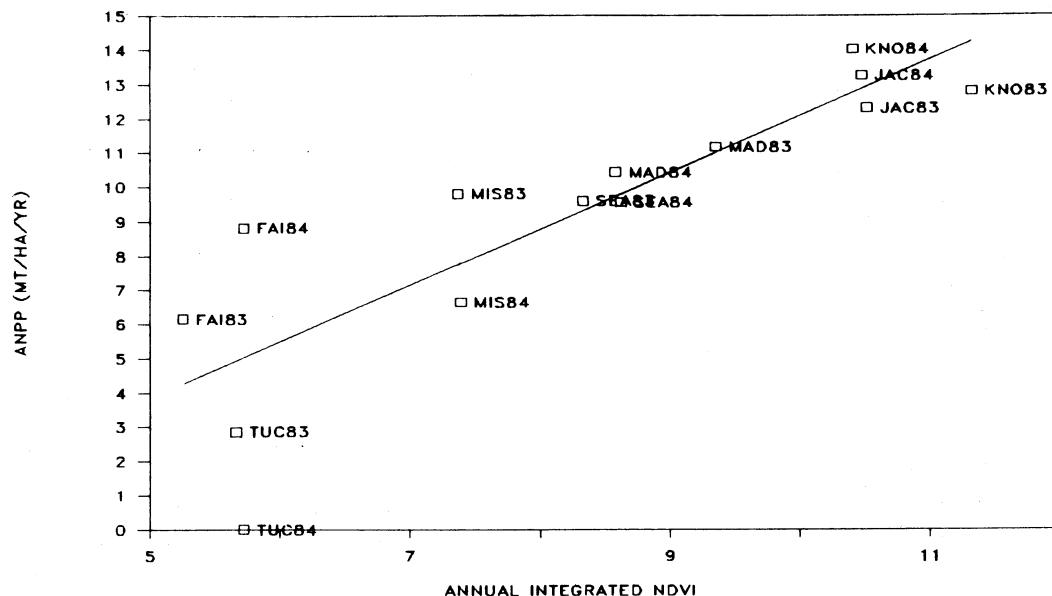


FIGURE 4. The correlation between annual integrated NDVI and annual aboveground net primary production (ANPP) in MT dry weight biomass calculated with the FOREST-BGC model for seven sites for the years 1983 and 1984. NDVI data were weekly composite spatially subsampled GVI data. The model simulated an annual carbon balance, including photosynthesis, maintenance and growth respiration and above/below ground carbon partitioning, and used a conversion of  $C \times 2.2 =$  dry weight biomass.  $Y = 1.64X - 4.35$ .  $R^2 = 0.72$ .

tal that these sites are also the most rigorously temperature and water limited for vegetation activity; influences of short-wave radiation on photosynthesis rates (and NDVI) do not predominate on these sites.

As stated in the methods section, the ANPP estimate from FOREST-BGC is strongly controlled by the biomass undergoing maintenance respiration and the above/below ground carbon partitioning ratio. Because only general estimates of these variables could be used for this simulation, actual ANPP values for mature forests at these sites could be  $\pm 30$ – $50\%$  of the values estimated in Fig. 4. However, the correlation of integrated annual NDVI vs. annual PSN from this study is quite similar to the correlation of integrated NDVI vs. NPP of natural vegetation estimated at an  $R^2 = 0.94$  by Goward et al. (1985). We conclude, as

did Goward et al., that these correlations are sufficient to suggest that integrated NDVI can significantly improve global estimates of annual vegetation productivity.

#### Weekly NDVI vs. photosynthesis

Given the strong correlation at an annual time scale between NDVI and PSN, we studied the seasonal trend of weekly results, expecting the differing climates to have some effect on correlations at shorter time scales. Figures 5–7 present results of the weekly NDVI and PSN trends for 1984 for all seven study sites, and Table 5 gives regressions of weekly NDVI on weekly PSN rates. The 1984 results contained the only complete annual trends of both variables, 1983 NDVI data were missing for the first 9 weeks of the year. For brevity the 1983 data is not pre-

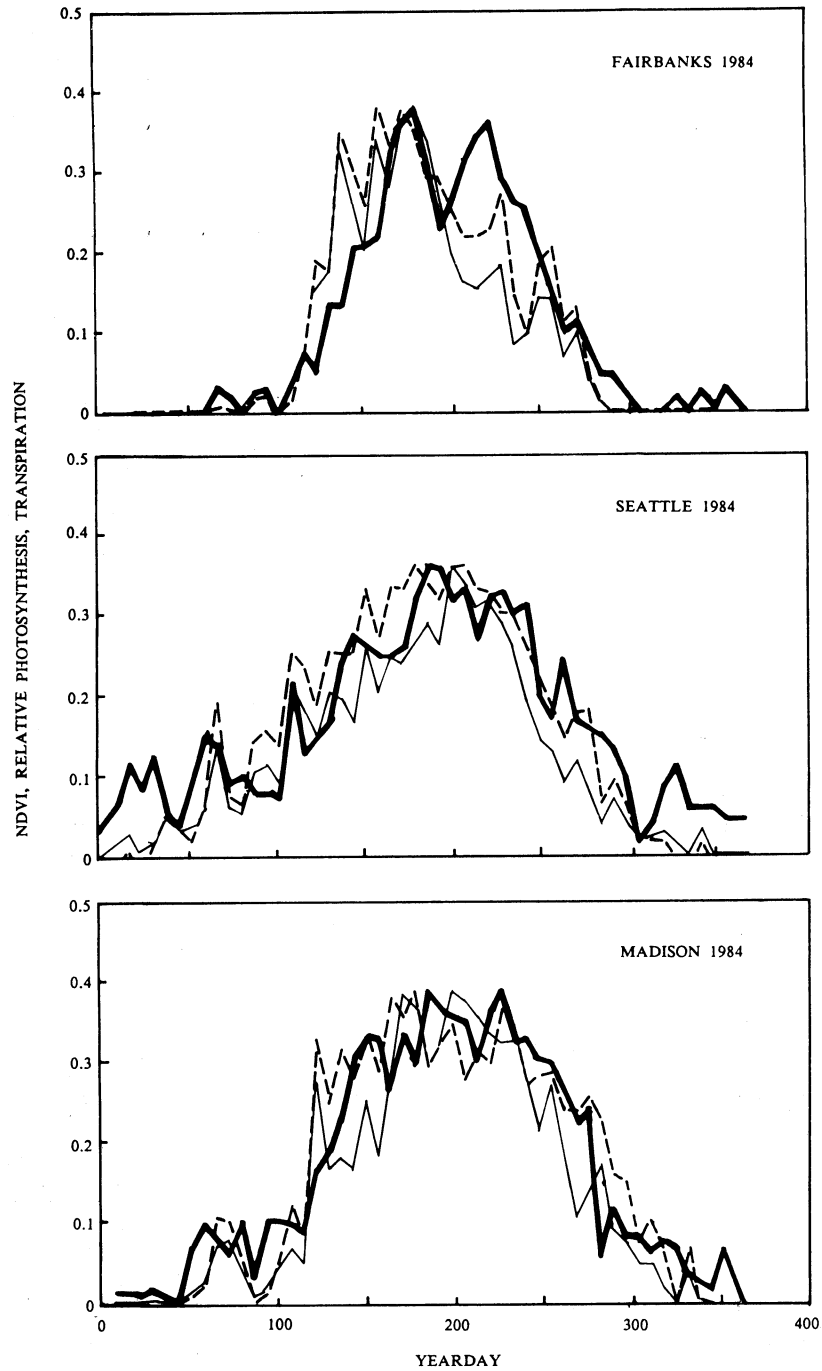


FIGURE 5. The seasonal trend of weekly composite NDVI (—) compared to scaled weekly sums of photosynthesis (PSN) (---) and transpiration (TRAN) (-·-) simulated by FOREST-BGC for three high latitude sites with a winter dormancy. Regression equations relating the three variables are shown in Table 5. The scaling factors were: for PSN, 2.08, 1.69, 1.75 MT carbon/ha/week/NDVI and, for TRAN, 63.9, 58.5, 52.3 mm/week/NDVI for Fairbanks, Seattle, and Madison, respectively.

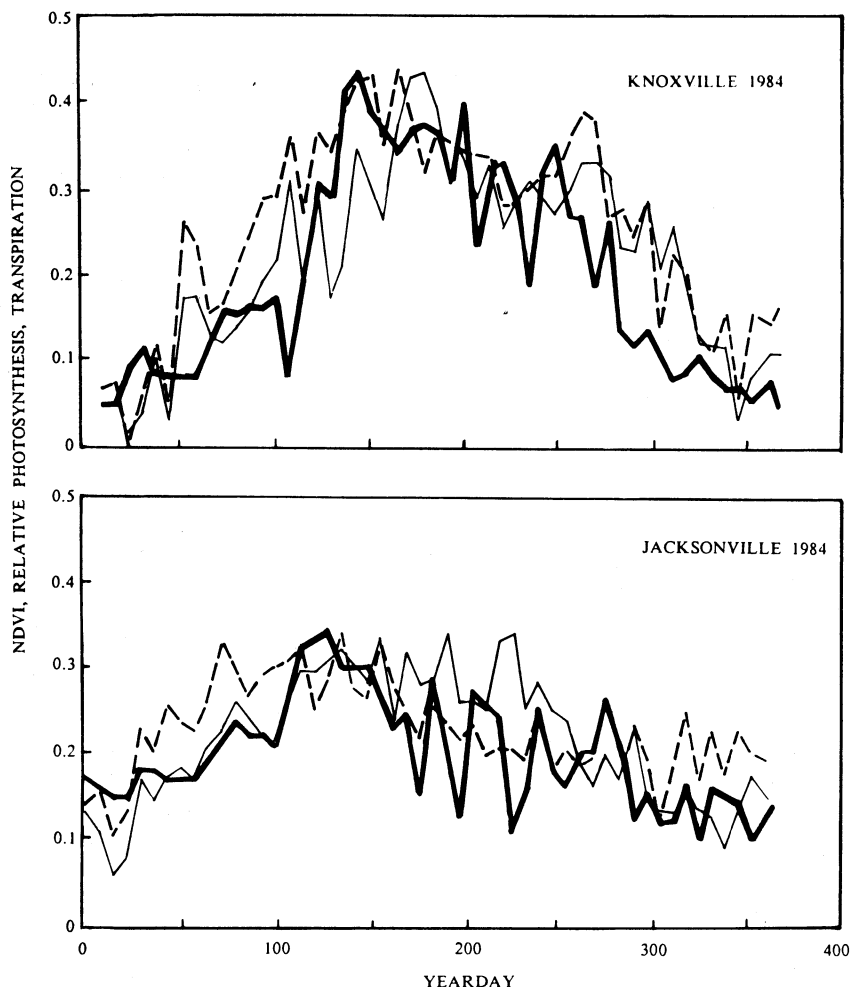


FIGURE 6. The seasonal trend of weekly composite NDVI (—) compared to scaled weekly sums of photosynthesis (PSN) (---) and transpiration (TRAN) (· · ·) simulated by FOREST-BGC for two low latitude sites with no water limitation and no winter subfreezing dormancy period. Regression equations relating the three variables are shown in Table 5. The scaling factors were: for PSN, 1.51, 1.78 MT carbon/ha/week/NDVI and, for TRAN, 46.1, 54.7 mm/week/NDVI for Knoxville and Jacksonville, respectively.

sented, but in no case does it contradict the trends and interpretations found in 1984.

Substantial variability in the correlation between NDVI and PSN is evident, from a high correlation of  $R^2 = 0.84$  at Madison, WI to a low of  $R^2 = 0.08$  at Tucson, AZ. However, most correlations were in the range of  $R^2 = 0.44$ – $0.84$  (Ta-

ble 5). The PSN results have been scaled to the NDVI results in Figs. 5–7 for direct comparison. In Table 5, a definite trend is evident, where sites with progressively less water availability produce less PSN per unit of NDVI, as evidenced by the decline in slopes of the PSN vs. NDVI regressions, from 1.99 to  $-0.86$ . This trend was tested by first creating an

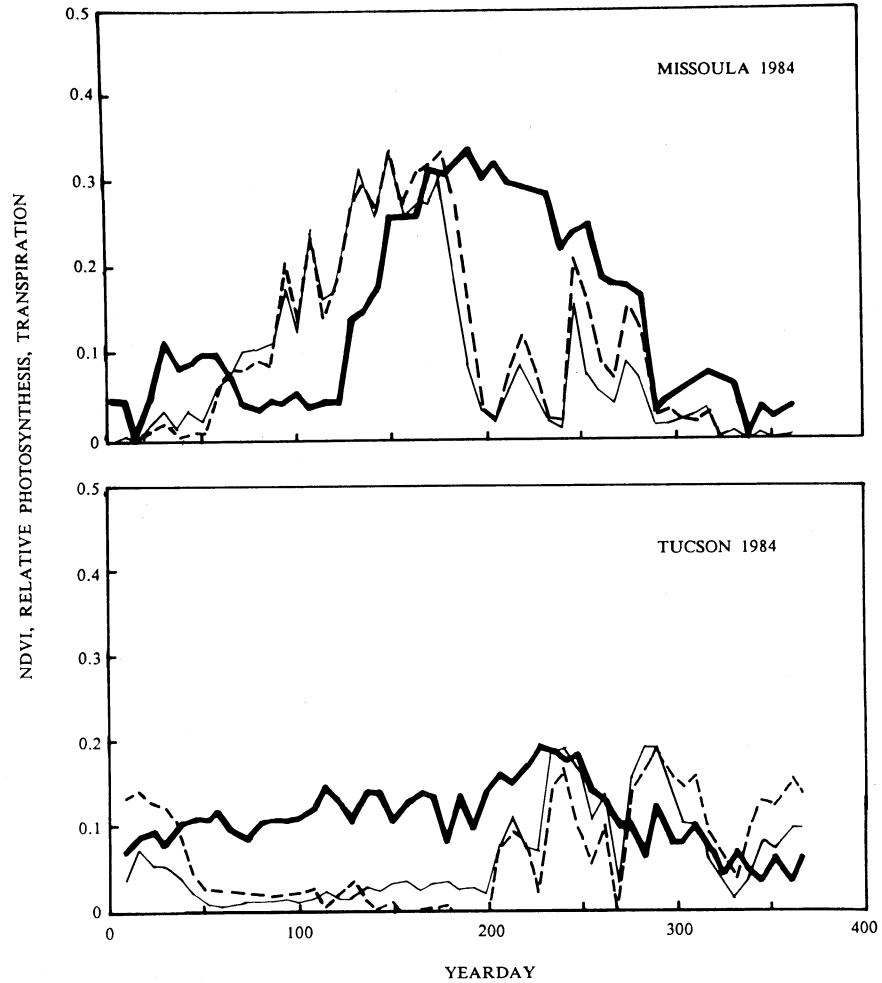


FIGURE 7. The seasonal trend of weekly composite NDVI (—) compared to scaled weekly sums of photosynthesis (PSN) (---) and transpiration (TRAN) (· · ·) simulated by FOREST-BGC for two sites with substantial seasonal vegetation water stress. The Missoula site has a substantial winter dormant period of air temperatures below 0°C, the Tucson site does not have a dormant period defined by air temperature. Regression equations relating the three variables are shown in Table 5. Scaling factors were: for PSN, 1.78, 1.85 MT carbon/ha/week/NDVI and, for TRAN, 48.1, 67.4 mm/week/NDVI for Missoula and Tucson, respectively.

“aridity index,” dividing annual radiation/annual precipitation for the 1984 meteorological data from each site from Table 4. This aridity index was regressed against the slope of the PSN/NDVI from Table 5. The regression found was  $Y = -0.16 * X + 2.24$ ,  $R^2 = 0.62$ , where  $X$  = the aridity index of radiation/precipita-

tion (in  $\text{MJ}/\text{m}^2 \text{ rad}/\text{mm H}_2\text{O}$ ), and  $Y$  = slope of the PSN/NDVI ratio in  $\text{MT C}/\text{ha}/\text{week}/\text{NDVI}$ . This result may suggest a useful means of scaling raw NDVI data to produce a better estimate of PSN over large areas using only general annual climatological data. Typically, during the midsummer when NDVI is

**TABLE 5** Regressions of Weekly NDVI against Weekly Photosynthesis and Transpiration Rates for Forests on the Seven Sites, for 1984<sup>a</sup>

SITE	EQUATION	CORRELATION
Fairbanks	PSN = 1.90 * NDVI + 0.012	$R^2 = 0.77$
	TRAN = 50.6 * NDVI + 0.33	$R^2 = 0.72$
Seattle	PSN = 1.99 * NDVI - 0.067	$R^2 = 0.81$
	TRAN = 56.4 * NDVI - 1.82	$R^2 = 0.82$
Missoula	PSN = 0.88 * NDVI + 0.066	$R^2 = 0.24$
	TRAN = 15.9 * NDVI + 2.45	$R^2 = 0.13$
Madison	PSN = 1.70 * NDVI + 0.039	$R^2 = 0.84$
	TRAN = 48.6 * NDVI - 0.84	$R^2 = 0.85$
Knoxville	PSN = 1.14 * NDVI + 0.016	$R^2 = 0.64$
	TRAN = 32.5 * NDVI + 3.68	$R^2 = 0.59$
Jacksonville	PSN = 1.01 * NDVI + 0.020	$R^2 = 0.44$
	TRAN = 41.0 * NDVI + 3.58	$R^2 = 0.39$
Tucson	PSN = - 0.86 * NDVI + 0.022	$R^2 = 0.08$
	TRAN = 14.6 * NDVI + 2.71	$R^2 = 0.02$

<sup>a</sup>PSN = MT<sup>1</sup>C/ha/week/NDVI; TRAN = mm/week/NDVI.

highest, the FOREST-BGC model is predicting PSN rates limited by leaf water stress and high vapor pressure deficits on water-limited sites.

For further interpretations, we combine analysis of these results into three groups. Fairbanks, Seattle, and Madison are all high latitude sites with strong seasonality to both NDVI and PSN, because of large seasonal amplitude of daylength and incident radiation. However, they are all climates with little seasonal water stress so that PSN is driven primarily by radiation and temperature, both controlled by the shortwave energy that the NDVI responds to. Consequently, the correlations are uniformly high,  $R^2 = 0.77-0.84$  between PSN and NDVI. Jacksonville and Knoxville are both lower latitude sites with less seasonality of NDVI and PSN, and periods of pronounced instability in the NDVI that we attribute to extended periods of cloudcover. For example, the week to week NDVI oscillations at Jacksonville around Yearday 200 (Fig. 6) are unlikely to be caused by fluctuating

forest leaf area, and the model suggests little fluctuation in weekly PSN. Vegetation leaf area simply cannot drop, regrow, and redrop over the course of 4 weeks.

In the third group, Missoula at a similar latitude to Seattle and Madison, is substantially water-limited throughout the late summer, so that correlations of PSN with NDVI are poor because NDVI does not respond to canopy water stress. The other substantially water limited site is Tucson, which showed a low NDVI with little seasonality because of the low latitude location and arid climate. Virtually no correlation of NDVI and PSN existed at Tucson because the FOREST-BGC model would respond to rainfall and water stress events with increasing then decreasing PSN while NDVI remained relatively constant.

Returning for more in depth analysis of the results, the three non-water-limited high latitude sites generally showed good correspondence in week to week oscillations of NDVI and PSN. These oscillations were presumably caused by heavy

cloudcover, reducing both NDVI and PSN, followed by clearer weather that increased both variables. Model results suggest that Seattle experienced mild water stress from Yeardays 230–300, but this late in the growing season sunangle caused the NDVI to rapidly drop also. The dramatic midsummer drop in both NDVI and PSN at Fairbanks was the result of 4 weeks of cloudy weather; both NDVI and PSN recovered briefly in late summer to high values before the sunangle and daylength controls on this 64° latitude site ended the growing season. The tight correspondence in spring and fall timing of the NDVI and PSN suggests that on these sites the NDVI does very well at defining growing season length. However, we suspect that the NDVI is responding to the seasonal phenology of grasses and broadleaf plants, not sensing photosynthetic activity directly. The GVI spatial subsampling scheme preferentially seeks bright NDVI targets such as grasses and broadleaves. We feel this logic increases the GVI sensitivity to the phenology of seasonal leaves, but may erroneously truncate estimates of photosynthetic activity of evergreen leaves.

The most methodical discrepancy between NDVI and PSN on the Jacksonville and Knoxville sites occurred in the spring during Yeardays 50–130. We consider the model to be in error here, because it assumes constant annual leaf area, and uses a night minimum temperature function of subfreezing temperatures to define growing season phenology. These sites have a substantial component of deciduous trees that would be leafless in early spring, yet have temperatures above freezing. Probably the NDVI tracks leaf development fairly accurately on these sites. This provides an example of where

future ecosystem models could be driven by satellite data, allowing improved temporal tracking of seasonal canopy development. Overestimation of PSN in the fall, particularly at Knoxville, is probably because the NDVI reacts to deciduous leaf drop while the model does not, again a point where satellite data driving an ecosystem model would have synergistic effects.

Correlation of NDVI and PSN on the Missoula site was lowest at two specific times of the year. In early spring, the model predicted high PSN beginning as snowmelt commenced, around Yearday 80, while NDVI accelerated about 7 weeks later. Both the NDVI and PSN results may partially be to blame. The model uses a constant leaf area index year around, and assumes no post-winter rebuilding of photosynthetic pigments and biochemistry, and so may overestimate early spring PSN. In fact, leaf growth of Montana evergreen forests begins around Yearday 130, and conifer leaves in cold winter climates have been found to require from 2 to 4 weeks to rebuild photosynthetic capacity after subfreezing winters (Larcher, 1980). Conversely, NDVI may climb slowly because of partial snowcover under the tree canopies increasing shortwave or Ch. 1 reflectance. Snowmelt is usually not complete until at least Yearday 150 in the midelevation forest area.

The FOREST-BGC model predicted substantial water stress on the Missoula site from Yearday 180 to 300, with pre-dawn leaf water potentials below  $-1.0$  MPa. We have documented this summer water stress period well by field measurements (Graham and Running, 1984; Donner and Running, 1986; Running, 1984), and so have confidence in the

**TABLE 6** Regressions of Weekly Transpiration against Weekly Photosynthesis for the Seven Study Sites in 1984<sup>a</sup>

SITE	EQUATION	CORRELATION
Fairbanks, AK	PSN = 0.035 * TRAN + 0.120	R <sup>2</sup> = 0.96
Seattle, WA	PSN = 0.034 * TRAN + 0.032	R <sup>2</sup> = 0.95
Missoula, MT	PSN = 0.039 * TRAN + 0.080	R <sup>2</sup> = 0.94
Madison, WI	PSN = 0.033 * TRAN + 0.470	R <sup>2</sup> = 0.88
Knoxville, TN	PSN = 0.030 * TRAN + 0.830	R <sup>2</sup> = 0.79
Jacksonville, FL	PSN = 0.015 * TRAN + 2.300	R <sup>2</sup> = 0.40
Tucson, AZ	PSN = 0.024 * TRAN + 0.220	R <sup>2</sup> = 0.61

<sup>a</sup>PSN = kg C/ha/week; TRAN = mm/week.

model prediction. The three small spikes of PSN and TRAN between Yeardays 230 and 280 are the result of rainfall temporarily alleviating water stress, but no response is evident in the NDVI.

In a previous paper (Running, 1986) it was suggested that NDVI might be corrected by surface temperature generated vapor pressure deficit calculations to improve the sensitivity of the NDVI to vegetation water stress. This correction procedure was tried in this study and produced results inferior to the uncorrected NDVI results, and so is not being presented. However, we are continuing to explore a correction procedure that would give the NDVI some sensitivity to vegetation water stress.

Interpretation of the Tucson results is particularly difficult. The model simulated seasonal dynamics of photosynthetic activity related to precipitation events that the NDVI does not register. Both Missoula and Tucson received 25% less precipitation in 1984 than in 1983 (Table 4). The FOREST-BGC model predicted reduced PSN of -25% at Missoula and -37% at Tucson in 1984, and yet the annual NDVI for both sites was unchanged from 1983 to 1984. Since the precipitation differences between years

are measured ground data, even those skeptical of the simulation results must conclude that the NDVI did not respond to these substantial drought conditions on the two sites. However, some of the Tucson site could be irrigated land, confounding this interpretation. Reliability of the NDVI for very arid sites with low vegetation cover has been questioned before (Malingreau, 1986).

#### Weekly NDVI vs. transpiration

Table 5 illustrates a similar trend between weekly NDVI and TRAN on progressively water-limited sites as PSN, as water is less available, a unit of NDVI produces less TRAN. Again we used the aridity index to quantify water availability in a general way, and regressed it against the slope TRAN/NDVI from Table 5. The result was a regression of  $Y = -2.96 * X + 58.0$ ,  $R^2 = 0.72$ , where  $X = \text{annual radiation/precipitation (in MJ/m}^2 \text{ rad/mm H}_2\text{O)}$  and  $Y = \text{slope TRAN/NDVI in mm H}_2\text{O/week/NDVI}$ . The regression was strongly influenced by Missoula and Tucson, with the slopes of the other sites within 1 standard deviation of a mean of 45.8 mm H<sub>2</sub>O/week/NDVI.

### Relationship of photosynthesis to transpiration

It is often implied that PSN is directly related to TRAN, and both processes to NDVI under specified conditions (Sellers, 1985). We explored the relationship by regressing weekly TRAN against weekly PSN for the seven sites for 1984 (Table 6). The correlation between PSN and TRAN ranged from a high of  $R^2 = 0.96$  at Fairbanks, to a low of  $R^2 = 0.40$  at Jacksonville. Although the regression slopes were reasonably similar for all sites except Jacksonville, PSN is not exactly related to TRAN, and the relationship changes in different climates.

Incident radiation drives PSN directly, almost linearly at  $LAI = 2.7$ , through the KM term in Eq. (1). However, radiation only weakly influences transpiration. A brief sensitivity analysis of the Penman-Monteith equation demonstrates that, given an air temperature of  $20^\circ\text{C}$ , high incident radiation of  $1000 \text{ W/m}^2$ , and a modest vapor pressure deficit of 10 mb, the radiation component of the transpiration driving force is only 9% of the total. Temperature drives PSN directly through the KM term also, and drives transpiration through the vapor pressure deficit. Canopy water deficit controls both PSN and TRAN similarly through the KL term. However, humidity deficit increases TRAN through the Penman-Monteith equation, yet decreases PSN through the KL control, having no effect on the PSN driving force. Consequently, cool, clear, high humidity spring days can produce high PSN rates but low TRAN rates. These conditions of optimal water use efficiency are evident in the springtime on all sites, and throughout much of the year in Seattle (Figs. 5-7). High radiation, high temperature, and high vapor

pressure deficit conditions tend to drive both processes about equally. Hot, cloudy summer days most evident in Jacksonville drive TRAN faster than PSN. However, generalizing about the complex, nonlinear controls of these processes is difficult, and illustrates the need for comprehensive process models for accurate calculations.

The correlations between PSN and TRAN, and NDVI can also be expected to be strong in climates where radiation is the primary control, because NDVI is related to reflected radiation. However, in climates where water stress and vapor pressure deficits progressively control PSN and TRAN, high correlations to NDVI cannot be expected.

### Conclusions

To our knowledge this is the first time the NDVI has been tested against a process level ecosystem simulation model, particularly down to time scales of 1 week. We find the results encouraging for use of NDVI for global scale comparisons of annual PSN, TRAN, and ANPP trends of forests in different climates. The strong relationship between integrated annual NDVI and NPP of natural vegetation found by Goward et al. (1985) appears corroborated. The prediction by Sellers (1985) from theoretical analysis that NDVI is directly related to photosynthesis in non-water-limited environments appears substantiated at regional scales.

However, we do not have confidence in use of the GVI to represent PSN, TRAN, and ANPP of specific sites over shorter times scales. To refine our understanding and utility of NDVI data, the next step of research should be based on LAC 1.1 km NDVI data with constant

geographic registration, avoiding the GVI subsampling system that leaves one not knowing what is really being imaged. Specific study sites can then be defined, and critical parameter estimates for the FOREST-BGC model such as LAI, soil water holding capacity, and leaf nitrogen concentration can be directly measured, which will improve our confidence in the ecosystem simulation results. Ground sampling at AVHRR pixel scales is a fundamental problem that may best be addressed by a hierarchy of measurements from ground to Landsat Thematic Mapper to AVHRR.

It is difficult to interpret the significance of the seasonal trends of NDVI. Coniferous forests do not show a seasonal change in leaf area equivalent to the NDVI seasonality exhibited by the Seattle or Missoula sites. We feel the GVI subsampling is biased toward bright annual leaves with strong seasonal phenology. An alternative hypothesis, which we consider unlikely, is that the NDVI is actually sensitive to canopy physiological activity. This hypothesis requires the controlled study suggested above to resolve.

At this point we think the best interpretation of integrated NDVI is as related to Leaf Area Duration, or LAI  $\times$  growing season length. LAD provides a simple but powerful measure of annual productivity that can be used to compare deciduous and coniferous forests. (See Waring and Schlesinger, 1985, p. 53, for a good analysis of LAD). With this logic, it becomes important to relate NDVI to LAI, and to define growing season in an ecologically accurate way, preferably by minimum temperature thresholds. However, NDVI seemed to provide a good measure of growing season in this study, perhaps because bright deciduous leaves that are

preferentially imaged by the GVI subsampling logic are phenologically controlled by freezing temperatures.

Finally, we offer the aridity index as an empirical means of correcting NDVI data for vegetation water stress effects on PSN and TRAN efficiency. However, we expect that further research will provide better means of correcting NDVI for vegetation stress effects. Further, we ultimately plan to use NDVI data to directly drive ecosystem process models such as FOREST-BGC. In that way, the strength of the satellite data for daily data collection can be coupled with the power of the computer simulation to calculate rates of processes that are invisible to an optical sensor.

*Funding for this study was provided by the National Aeronautics and Space Administration, Earth Sciences and Applications Division, Grant No. NAGW-952, Joint Research Interchanges Nos. NCA 2-138 and NCA 2-27 from the NASA Ames Research Center, Moffett Field, CA, and McIntire-Stennis funding to the University of Montana. Particular thanks goes to David L. Peterson for offering detailed interpretation of the results. We thank Drs. Joe Landsberg, Trevor Booth, Ross McMurtrie, and Gavin Byrne for reviews of the draft manuscript. This research was completed while the senior author was a visiting scientist at the CSIRO Division of Forest Research, Canberra, Australia.*

## References

- Bristow, K. L., and Campbell, G. S. (1984), On the relationship between incoming solar radiation and daily maximum and minimum temperature. *Agric. Forest Meteorol.* 31:159-166.

- Dahlman, R. C. (1985), Modeling needs for predicting responses to CO<sub>2</sub> Enrichment: plants, communities and ecosystems, *Ecol. Modeling* 29:77-106.
- Donner, B. L., and Running, S. W. (1986), Water stress response after thinning *Pinus contorta* stands in Montana, *Forest Sci.* 32:614-625.
- Emmanuel, W. R., Killough, G. G., Post, W. M., and Shugart, H. H. (1984), Modelling terrestrial ecosystems in the global carbon cycle with shifts in carbon storage capacity by land-use change, *Ecology* 65:970-983.
- Fung, I. Y., Tucker, C. J., and Prentice, K. C. (1987), Application of AVHRR Vegetation Index to study atmosphere-biosphere exchange of CO<sub>2</sub>, *J. Geophys. Res.*, forthcoming.
- Goward, S. N., and Dye, D. G. (1987), Evaluating North American net primary productivity with satellite observations, *Adv. Space Res.*, forthcoming.
- Goward, S. N., Tucker, C. J. and Dye, D. G. (1985), North American vegetation patterns observed with the NOAA-7 advanced very high resolution radiometer, *Vegatatio* 64:3-14.
- Graham, J. S. and Running, S. W. (1984), Relative control of air temperature and water status on seasonal transpiration of *Pinus contorta*, *Can. J. Forest Res.* 14:833-838.
- Holben, B. N. (1986), Characteristics of maximum value composite images from temporal AVHRR data, *Int. J. Remote Sens.* 7:1417-1434.
- Kidwell, K. B. (1984), NOAA polar orbital data users guide (TIROS-N, NOAA-6, -7, -8), NOAA National Climate Center, Washington, DC.
- Larcher, W. (1980), *Physiological Plant Ecology*, 2nd ed., Springer-Verlag, Berlin, 303 pp.
- Justice, C. O., Townshend, J. R. G., Holben, B. N., and Tucker, C. J. (1985), Analysis of the phenology of global vegetation using meteorological satellite data, *Int. J. Remote Sens.* 6:1271-1318.
- Malingreau, J. P. (1986), Global vegetation dynamics: satellite observations over Asia, *Int. J. Remote Sens.* 7:1121-1146.
- Running, S. W. (1984), Microclimate control of forest productivity: Analysis by computer simulation of annual photosynthesis/transpiration balance in different environments, *Agric. Forest Meteorol.* 32:267-288.
- Running, S. W. (1986), Global primary production from terrestrial vegetation: Estimates integrating satellite remote sensing and computer simulation technology, *Sci. Total Environ.* 56:233-242.
- Running, S. W., and Coughlan, J. C. (1987), A general model of forest ecosystem processes for regional applications. I. Hydrologic balance, canopy gas exchange and primary production processes. *Ecol. Modelling*, forthcoming.
- Running, S. W., Peterson, D. L., Spanner, M. A., and Teuber, K. B. (1986), Remote sensing of coniferous forest leaf area, *Ecology* 67:273-276.
- Running, S. W., Nemani, R. R., and Hungerford, R. D. (1987), Extrapolation of synoptic meteorological data in mountainous terrain, and its use for simulating forest evapotranspiration and photosynthesis, *Can. J. Forest Res.* 17:472-483.
- Sellers, P. J. (1985), Canopy reflectance, photosynthesis and transpiration, *Int. J. Remote Sens.* 6:1335-1372.
- Sellers, P. J. (1987), Canopy reflectance, photosynthesis and transpiration. II. The role of biophysics in the linearity of their interdependence, *Remote Sens. Environ.* 21:143-183.
- Tarpley, J. D., Schneider, S. R., and Money, R. L. (1984), Global vegetation indices from the NOAA-7 meteorological satellite, *J. Clim. Appl. Meteorol.* 23:491-494.

- Tucker, C. J. (1980), Remote sensing of leaf water content in the near infrared. *Remote Sens. Environ.* 10:23-32.
- Tucker, C. J., Townshend, J. R. G., and Goff, T. E. (1985), African landcover classification using satellite data, *Science* 227: 369-375.
- Tucker, C. J., Fung, I. Y., Keeling, C. D., and Gammon, R. H. (1986), Relationship between atmospheric CO<sub>2</sub> variations and a satellite-derived vegetation index, *Nature* 319:195-199.
- Waring, R. H., and Schlesinger, W. H. (1985), *Forest Ecosystems: Concepts and Management*, Academic, New York, 340 pp.
- Webb, W. L., Lauenroth, W. K., Szarek, S. R., and Kinerson, R. S. (1983), Primary production and abiotic controls in forests, grasslands, and desert ecosystems in the United States, *Ecology* 64:134-151.
- Wittwer, S. (Chair) (1983), Land related global habitability science issues, NASA Tech. Mem. 85841, 112 pp.

Received 7 May 1987; revised 31 July 1987.